Surface Science 603 (2009) 1571–1578

Contents lists available at ScienceDirect

Surface Science

journal homepage: www.elsevier.com/locate/susc

Nonadiabatic quasiparticle dynamics in time resolved electron spectroscopies of surface bands

Predrag Lazić [a,1], Damir Aumiler [b,2], Branko Gumhalter [c,*]

[a] Institut für Festkörperforschung, Forschungszentrum Jülich, D-52425 Jülich, Germany
[b] State Key Laboratory of Molecular Reaction Dynamics, Institute of Chemistry, Chinese Academy of Sciences, Beijing, China
[c] Institute of Physics, HR-10000 Zagreb, Croatia

ARTICLE INFO

Article history:
Available online 20 January 2009

Keywords:
Electron states at surfaces and interfaces
Two-photon photoemission and photoelectron spectra
Time resolved optical spectroscopy
Nonadiabatic electron dynamics
Decoherence and decay of surface electronic states
Ultrafast quasiparticle relaxation
Optical Bloch equations parameterization

ABSTRACT

Surface localized electronic states constitute electronic environment for a variety of physical and chemical phenomena taking place on surfaces. Various processes of model catalytic reactions may be influenced or mediated by hot electrons and holes excited in quasi-two-dimensional bands occurring on a large number of metal surfaces. Here we discuss several important aspects of nonadiabatic dynamics of these excitations which may affect the measurements of surface electronic properties by ultrafast electron spectroscopies.

© 2009 Elsevier B.V. All rights reserved.

1. Introduction

Research in the field of heterogeneous catalysis is truly interdisciplinary and covers many areas of physics, chemistry and materials science. In this short review we shall attempt to elucidate some aspects of ultrafast surface electron dynamics which may play important roles in the various surface phenomena, including the catalytic reactions at gas-solid interfaces.

Catalytic reactions on solid surfaces can be viewed as sequences of chemical bond breakings and makings involving the reactant, transition or intermediate, and product species in interaction with the catalyst surface. These events are characterized by electronic transitions from ground or excited states of the initial molecular configurations of reactants, via the excited states of intermediates, to the final molecular configurations of product species. During these processes substantial amounts of excited electron energies can be transferred to the other dynamical degrees of freedom in the reacting system or dissipated to the heatbath. Various surface science techniques and methods have been developed and employed to study the electronic structure of real and model catalyst surfaces *per se*, and of the reactants and products in interactions with catalyst surfaces. The primary goal of these investigations was to obtain physical and chemical insight into the various stages of studied reactions on well characterized surfaces and thereby assess the corresponding driving potentials and reaction pathways [1–4].

Studies of model catalytic surfaces and their interactions with prototype adsorbates represent a broad research area in which the activities can be traced back to the very beginnings of surface science. Investigations of the electronic properties of clean and adsorbate covered crystal surfaces by various electron spectroscopies constitute an important chapter in this endeavor (for review and exhaustive list of references see contributions to this volume by G.A. Somorjai, C. Campbell, M. Wolf et al., F. Besenbacher, A. Jablonski, and Ref. [5]). This particularly refers to the surfaces of noble and transition metals which have proven as or are deemed to be efficient catalysts in a variety of reactions of practical and scientific interest. Single crystal metal surfaces represent electronic environments for model catalytic reactions whose properties are nowadays accessible by standard and novel surface science techniques. Applications of these techniques can provide spatially-, temporally- and energy-resolved information on the electronic structure and dynamics of participants in the various surface mediated processes [7]. The broad range and high resolution of the acquired data have in many cases enabled to establish microscopic descriptions of the dynamics of electronic and nuclear degrees of freedom during the various stages of surface reactions (see G. Ertl's Nobel Lecture at http://nobelprize.org/nobel_prizes/chemistry/laureates/2007/ertl-lecture.html).

* Corresponding author. Fax: +385 1 469 8889.
E-mail address: branko@ifs.hr (B. Gumhalter).
[1] Permanent address: Rudjer Bošković Institute, Zagreb, Croatia.
[2] Permanent address: Institute of Physics, Zagreb, Croatia.

0039-6028/$ - see front matter © 2009 Elsevier B.V. All rights reserved.
doi:10.1016/j.susc.2008.09.061

The majority of low index single crystal surfaces of catalytically active noble and transition metals support quasi-two-dimensional (Q2D) surface localized electronic bands. Surface bands around the Fermi and vacuum level arise from a combined action of the attractive image potential and the projection(s) of bulk band gap(s) in the direction perpendicular to the surface [6]. Hence, the electronic environment on a number of catalyst surfaces may be affected by Q2D band structure and concomitant electron dynamics. Of particular importance in the context of surface interactions and reactions is the dynamics of Q2D electronic states on the ultrashort time scale of chemical bond making and bond breaking which is in the range of femtoseconds. The dynamics of surface electrons on this scale is also expected to influence many other surface phenomena such as the electronic and spin response properties of adlayers and nanostructures, the speed and quality of information storage and retrieval needed for the design of future quantum computing devices, etc. Therefore it is of special interest to study the electronic properties and response of paradigmatic model systems of reduced dimensionality such as surface bands in order to gain fundamental understanding of electron dynamics subject to spatial and temporal confinement. A lot of effort has been devoted to develop experimental techniques which would accomplish these goals and recent applications of ultrafast photoelectron spectroscopies have enabled high resolution studies of electron dynamics at surfaces in the real time domain. This provided novel insights into the evolution and decoherence of surface-localized electronic states and opened up new directions in the investigations of surface interactions and reactions on the ultrashort time scale.

Many important aspects of hot charge carrier energetics and dynamics in surface-localized bands have been successfully explored by high resolution one-photon-photoemission (1PPE) spectroscopy [8–12], inverse photoemission (IPE) spectroscopy [13], scanning tunneling microscopy [14,15] (STM), and two-photon-photoemission (2PPE) combining the use of continuous wave (cw) and pulsed pump and probe laser beams with variable delay times [16–30]. Time resolved two-photon-photoemission (TR2PPE) studies of surfaces with ultrashort laser pulses have provided particularly valuable information on quasiparticle dynamics in surface bands which is one of the prerequisites for a better understanding of surface photochemistry. Systematic applications of these methods have resulted in accumulation of the data on characteristic energies and lifetimes of hot electron and hole excitations in Shockley and image potential bands on clean surfaces (hereafter to be referred to as the SS- and IS-bands, respectively), and in the states at surfaces covered with localized defects [31–36] such as adsorbates, cavities, steps, etc. Recent progress in interferometric 2PPE measurements has further enhanced the quality of information on the quasiparticle dynamics at surfaces [24–27].

The majority of theoretical descriptions and interpretations of evolution of quasiparticles created in surface bands during the various stages of spectroscopic measurements have been restricted to the adiabatic or Markovian (quasistationary) picture of hot carrier dynamics. In this approximation the evolution of quasiparticle states is characterized by exponential decay governed by the Fermi golden rule (FGR) type of transition rates [37–39]. Such a description is applicable to steady state evolution of the system during the times that are of the order of or exceed its relaxation and decay times. This regime was tacitly assumed in recent developments of microscopic theories of 2PPE from surface [40–43] and bulk [44] bands. The applicability of phenomenological optical Bloch equations in the simulations of time resolved 2PPE experiments [22,23,30,43,45–47] also rests on this assumption. However, time resolved 2PPE measurements utilizing pump and probe laser pulses of femtosecond duration and short delay times also probe the early non-Markovian evolution of quasiparticles excited in surface bands. Besides the possible direct consequences on the measured time resolved and interferometric 2PPE spectra, this fact may turn out important in the determination of 2PPE correlation traces since in that case the delay times are varied from negative to positive values across zero, in which case the non-Markovian and Markovian evolution of excited quasiparticles may equally contribute to the results of measurements.

In this article we illustrate the main characteristics of nonadiabatic evolution of hot electrons and holes excited in surface bands which are caused by the most common and ubiquitous interactions of quasiparticles with the environment, viz. the interactions with electronic charge density fluctuations in the system and with the impurity defects (adsorbates) present on the surface. Special attention will be paid to the discussion of quasiparticle features that may be used for identification of non-Markovian evolution regimes, namely the decay of survival probability of a quasiparticle and the evolution of its phase in the course of time. Their temporal variations on the ultrashort time scale are expected to leave important signatures in the spectral characteristics of surface bands revealed by ultrafast electron spectroscopies.

2. Amplitudes and intensities of one- and two-photon photoemission from surface bands

To illustrate how ultrafast electron dynamics enters model descriptions of the energy and time resolved one- and two-photon photoemission intensities from surface bands we shall employ time-dependent perturbation theory to describe interactions of electrons with ultrashort laser pulses. In the case of 1PPE from surface bands a laser pulse excites electrons from initially occupied band states below the Fermi energy E_F into final states $|k\rangle$ above the vacuum level $E_V = 0$. The states $|k\rangle$ are outgoing photoemission states in which the electron energy and emission angle can be measured by a suitable electron counter (hereafter to be referred to as the detector). This measurement defines the quantum numbers of the final photoelectron state $|k\rangle$ outside the solid, i.e. the photoelectron total energy E_k and the momentum parallel to the surface. We further assume that the detector plays the role of a projector operator, $\widehat{P}_f$, that in an idealized situation selects photoemitted electrons in the outgoing states $|k\rangle$, viz.

$$\widehat{P}_f = \sum_{k_f} |k\rangle\langle k|. \tag{1}$$

Here the summation over the indices k_f of photoelectron final states is restricted by the angular and energy resolution of the detector. The electron population of the states $|k\rangle$ in this interval at the instant of measurement t_{obs} (hereafter to be referred to as the observation time) is given by:

$$\rho_f(t_{\mathrm{obs}}) = \langle \Psi(t_{\mathrm{obs}})|\widehat{P}_f|\Psi(t_{\mathrm{obs}})\rangle, \tag{2}$$

where $|\Psi(t_{\mathrm{obs}})\rangle = U(t_{\mathrm{obs}}, -\infty)|\Psi(-\infty)\rangle$ is a many-body wave function of the system obtained by the action of evolution operator $U(t_{obs}, -\infty)$ on the initial ground state of the system $|\Psi(-\infty)\rangle = |0\rangle$ at $t = -\infty$. Here one should observe a difference with respect to the standard definition of photoemission yields based on current–current correlation functions [48–50] which is applicable to steady-state photoemission induced by stationary photon fields.

In the case of one-photon photoemission the operator $U(t_{obs}, -\infty)$ is calculated in first order perturbation theory with respect to the applied electromagnetic field of the laser pulse. This yields $\rho_f(t_{\mathrm{obs}})$ corresponding to the population induced by 1PPE process. Both the photoexcited electron in the state $|k\rangle$ and the hole left in the initial electron state may interact with each other and with the dynamical degrees of freedom of the system heatbath. These interactions will give rise to decoherence of primary coherent photoexcited electron-hole pair.

In the case of 2PPE from surface bands we assume that the first femtosecond laser pulse (pump) excites electrons from states in the occupied part of SS-band into intermediate unoccupied states in one of the IS-bands (for simplicity of presentation the excitations into other bands or states above E_V will be neglected and only the intuitive order of photoexcitation of electrons by the pump and probe pulses will be considered). Likewise the situation in 1PPE, the photoexcited hot electron and the hole left in the initial electron state may interact with each other and with the system heatbath, causing the decoherence of the primary excitation. The second laser pulse (probe) which is delayed by the time τ_{2PPE} relative to the pump pulse may then excite electrons from intermediate states into a final photoemission state $|k\rangle$ above E_V. To model this process $U(t_{obs}, -\infty)$ must be calculated in second order perturbation theory with respect to the applied electromagnetic field given by the sum of pump and probe pulses. This yields $\rho_f(t_{obs})$ corresponding to the population induced by the 2PPE process.

Finally, in the case of interferomentric 2PPE + 1PPE experiments $U(t_{obs}, -\infty)$ should be calculated in the presence of all three pulsed photon fields. In this situation the quantum mechanical amplitudes of photoelectrons from 2PPE and 1PPE channels may strongly interfere which should have a strong effect on the population of final states given by expression (2).

Since the temporal resolution of electron detectors is in the range of picoseconds, i.e. much longer than the duration of laser pulses and the relaxation times typical of the system [23] (that are all in the femtosecond range), the 1PPE, 2PPE and interferometric experiments will effectively measure the integrated quantity

$$\rho_f = \int dt_{obs}\rho_f(t_{obs}) = \int dt_{obs}\langle\Psi(t_{obs})|\widehat{P}_f|\Psi(t_{obs})\rangle$$
$$= \int dt_{obs}\sum_{k_f}\langle\Psi(t_{obs})|k\rangle\langle k|\Psi(t_{obs})\rangle. \quad (3)$$

Here the integration over t_{obs} can be extended throughout the interval $(-\infty, \infty)$ in view of the temporal localization of photoemission events induced by ultrashort pulses and fast quasiparticle decay relative to temporal resolution of the detector. In the case of high *energy* resolution of the detector one may substitute $\sum_{k_f}|k\rangle\langle k| \to N(E_f)|f\rangle\langle f|$ where $N(E_f)$ is the density of final electron states at energy E_f, and thereby obtain

$$\rho_f = N(E_f)\int_{-\infty}^{\infty} dt_{obs}\langle\Psi(t_{obs})|f\rangle\langle f|\Psi(t_{obs})\rangle. \quad (4)$$

Note that the photoexcited electron state from the many-body wavefunction $|\Psi(t_{obs})\rangle$ in the integrand on the RHS of expression (4) is projected onto the final photoelectron state $|f\rangle$ whereas all remaining many-body degrees of freedom are summed over since the electron counter does not detect other quasiparticles or heatbath excitations (i.e. the operator $\widehat{P}_f$ does not project them out onto any measured final state). Therefore, $\langle f|\Psi(t_{obs})\rangle$ is a coherent sum of photoemission amplitudes over all allowed intermediate state channels. For the sake of simplicity of presentation we shall in the following assume translationally invariant surfaces so as that the quantum states of electrons residing in surface bands will be denoted by $|\mathbf{K}, n\rangle$ where $\mathbf{K}$ is the quasiparticle momentum parallel to the surface and n is the band index (n = SS for surface state band, n = IS for the first image potential band, $n = k_z$ for a bulk band, etc.). Surface translational invariance also implies conservation of parallel momentum in 1PPE and 2PPE transition matrix elements because the momentum of exciting photons is negligible. Hence, the quantity $\langle\Psi(t_{obs})|f\rangle\langle f|\Psi(t_{obs})\rangle$ represents an incoherent sum over all possible initial states of the system that may partake in photoemission and thereby it reveals the initial electronic density of states.

The $|f\rangle$-resolved photoemission amplitudes

$$A_f(t_{obs}) = \langle f, other|\Psi(t_{obs})\rangle \quad (5)$$

in which *other* denotes quantum numbers of all other degrees of freedom of the system that are not detected at the instant t_{obs}, can be conveniently represented by sums of Feynman diagrams [51]. In the following we shall assume only one hot electron-hole pair propagating subsequent to each photon absorption, i.e. the Tamm-Dancoff approximation for the primary excited electron-hole pairs. Then, in the case of photoemission involving the initial SS- and intermediate IS-band states the corresponding diagrams are expressed in terms of the final state f-electron propagator or Green's function $G_f(t)$, intermediate state IS-electron propagator $G^{IS}_{\mathbf{K}}(t)$, initial state SS-hole propagator $G^{SS}_{\mathbf{K}}(t)$, and the propagators describing bosonized excitations of the system heatbath that couple to the excited hot quasiparticles. Typical higher order diagrams from these sums are shown in Fig. 1 for 1PPE (top panel) and 2PPE (bottom panel). They comprise both the self-energy and vertex corrections to the elementary processes whose diagrams are obtained by removing all the wiggly lines representing the heatbath excitations from the diagrams in Fig. 1. Earlier many-body studies of 1PPE from surfaces [52] have shown that selfenergy renormalizations of the hole propagators dominantly determine photoemission lineshapes and yields. Hence, the leading contribution to the 1PPE amplitude is given by the expression

$$A_f^{(1PPE)}(t_{obs}) = (-i)\int_{-\infty}^{t_{obs}} dt_1 G_f(t_{obs}-t_1)E^{1PPE}(t_1)G^{SS}_{\mathbf{K}}(t_{obs}-t_1), \quad (6)$$

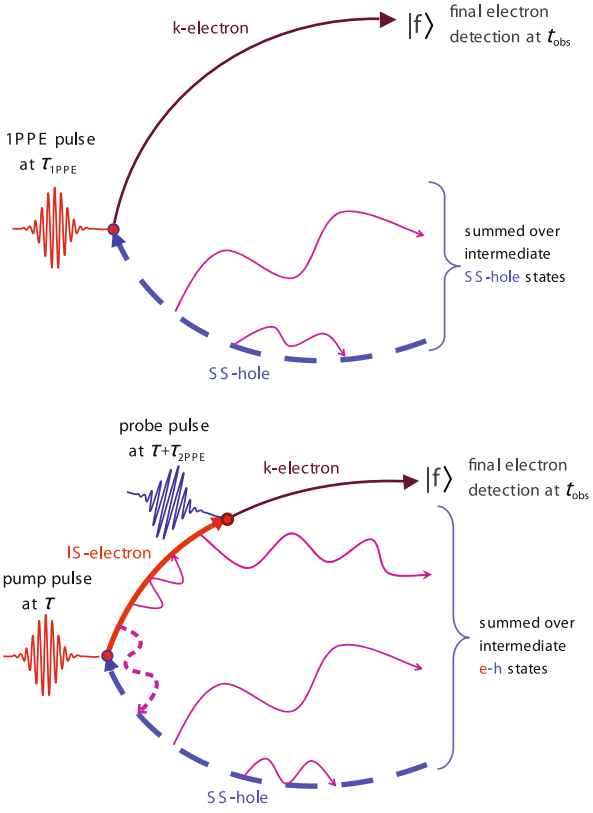

Fig. 1. Top: schematic of contributions to the amplitude of 1PPE from a surface state (SS) band. Thick dashed and thin full lines denote the SS-hole and electron propagator in a final photoelectron state above E_V, respectively, and wiggly lines illustrate excitations of the heatbath (for corresponding propagator representation of these lines see Appendix A of Ref. [51]). Electron–photon field interaction matrix element is denoted by a filled circle. Bottom: same for the amplitude of 2PPE from a SS-band via the intermediate IS-band band channel(s). Thick full line denotes the IS-electron propagator. Dashed wiggly line denotes Coulomb interaction between IS-electron and SS-hole that is dynamically screened by bosonized excitations of the heatbath which are represented by full wiggly lines. Pump and probe photon pulses are delayed by the time interval τ_{2PPE}. The counterintuitive order of the interactions with laser pulses, viz. $|SS\rangle \to |IS\rangle$ excitation by the probe and photoemission $|IS\rangle \to |k\rangle$ by the pump is not shown. In both pictures the photoelectron terminates in the final state $|f\rangle$ at the observation time t_{obs}.

where $E^{1PPE}(t_1)$ describes electron interaction with the applied pulsed photon field temporally localized around τ_{1PPE} and G_f and $G^{SS}_{\mathbf{K}}$ are the self-energy renormalized quasiparticle propagators (cf. Fig. 1).

Assessments of lowest order self-energy and vertex renormalizations of 2PPE amplitudes, which arise from the interactions of quasiparticles with dynamical degrees of freedom of the heatbath, have shown [53] that in the femtosecond range the IS–SS vertex corrections make a small correction relative to the contribution from self-energy renormalizations of the IS-electron and SS-hole propagators. Therefore, the leading contribution to 2PPE amplitude is given in terms of renormalized propagators

$$A_f^{(2PPE)}(t_{obs}) = (-i)^2 \int_{-\infty}^{t_{obs}} dt_2 G_f(t_{obs}-t_2) E^{pr}(t_2) \times \int_{-\infty}^{t_2} dt_1 G^{IS}_{\mathbf{K}}(t_2-t_1) E^{pu}(t_1) G^{SS}_{\mathbf{K}}(t_{obs}-t_1). \quad (7)$$

Here $E^{pu}(t_1)$ and $E^{pr}(t_2)$ describe electron interactions with electromagnetic fields of the pump and probe laser pulses temporally localized around τ and $\tau+\tau_{2PPE}$, respectively (cf. Fig. 1). In the case of more than one intermediate IS-band expression on the RHS of (7) should be summed over all intermediate state bands. Likewise the case of 1PPE from surface bands, the f-electron propagator is assumed unrenormalized in view of the much weaker interactions of delocalized outgoing electrons with the heatbath if photoelectron kinetic energies largely exceed the energies of heatbath excitations.

The retarded single particle propagators or Green's functions appearing in expression (7) are defined by

$$G^{SS}_{\mathbf{K}}(t_{obs}-t_1) = \langle 0|c^{\dagger}_{\mathbf{K},SS}(t_{obs}) c_{\mathbf{K},SS}(t_1)|0\rangle \theta(t_{obs}-t_1), \quad (8)$$

$$G^{IS}_{\mathbf{K}}(t_2-t_1) = \langle 0|c_{\mathbf{K},IS}(t_2) c^{\dagger}_{\mathbf{K},IS}(t_1)|0\rangle \theta(t_2-t_1), \quad (9)$$

$$G_f(t_{obs}-t_2) = \langle 0|c_f(t_{obs}) c^{\dagger}_f(t_2)|0\rangle \theta(t_{obs}-t_2), \quad (10)$$

where $c^{\dagger}_b(t')$ and $c_b(t')$ are the creation and annihilation operators in the Heisenberg picture, respectively, for an electron in the band state $|b\rangle = |\mathbf{K}, n\rangle$ or in the final photoemission state $|b\rangle = |f\rangle$, and $|0\rangle$ denotes the initial state of the system. Analogous expressions for Green's functions appear in Eq. (6). The time evolution or renormalization of propagators (8) and (9) should be calculated in the presence of interactions that dominantly affect the decay and decoherence of quasiparticles excited in surface bands. With these definitions and simplifying assumptions the major contributions to final state populations in 1PPE and 2PPE from surface bands are obtained by taking the absolute square of expression (6) or (7), respectively, and summing it over all other degrees of freedom. Analogously, the total amplitude in an interferometric experiment is then given by

$$A_f^{(intf)}(t_{obs}) = A_f^{(2PPE)}(t_{obs}) + A_f^{(1PPE)}(t_{obs}), \quad (11)$$

and its absolute square summed over all other degrees of freedom measures the photoemission induced population of the final states $|f\rangle$ that is affected by the interference of 2PPE and 1PPE electron excitation paths.

3. Survival probabilities and phase relaxations of quasiparticles in surface bands

Inspection of expressions (6) and (7) shows that the population of final photoelectron states in time resolved 1PPE and 2PPE from surface bands depends dominantly on the shapes of pulsed laser fields that determine the perturbations $E(t)$ and the excited quasiparticle dynamics embodied in the propagators $G^n_{\mathbf{K}}(t)$. Analyses of pulse characteristics and their effects on the 2PPE spectra were studied within a Markovian description of quasiparticle dynamics in Ref. [45]. In this section we complement these studies with the analyses of non-Markovian dynamics of quasiparticles excited in surface bands that may prove important for the interpretations of results of ultrafast spectroscopic measurements, particularly of 2PPE and interferometric photoemission from surfaces.

In the above described spectroscopic measurements the information on the electronic structure and dynamics of the system is obtained from the processes of electron injection into or removal from the quantum states of the probed system[3]. Nonadiabatic addition or removal of electrons induces the system response to the creation of uncompensated charges and spins and thereby to the dressing of excited hot electrons and holes into quasiparticles. Additional dressing of excited particles may also arise from their interactions with surface defects.

Non-Markovian dynamics of hot quasiparticles can be conveniently characterized by temporal evolution of the two quantities referred to at the end of Section 1, the survival probability $L_b(t)$ of the quasiparticle initial state $|b\rangle$, and the total phase $\phi_b(t)$ of its propagation amplitude. They are obtained as:

$$L_b(t) = |G_b(t)|^2, \quad (12)$$

$$\phi_b(t) = -Im \ln G_b(t), \quad (13)$$

where b stands for the quantum numbers $(\mathbf{K}, n)$ appearing in Eqs. (8) and (9). Survival probabilities and phases of quasiparticles in Q2D surface bands are controlled by interactions with the environment. Here we shall discuss interactions with charge density response of the system and with localized surface defects (adsorbates), which are the two most common and most investigated sources of quasiparticle decay and decoherence at metal surfaces.

3.1. Effects of quasiparticle interactions with the charge density excitations

Quasiparticle interactions with the electronic charge density fluctuations in the system will be described in the dynamic response formalism in which central quantity is the linear response function χ of metal electrons [51,59] whose excitations may range over the bulk bands as well as over the surface bands that arise from the combined effect of the surface projected bulk band gaps and surface localized image potential U_{im}. The thus introduced U_{im} corresponds to exchange-correlation correction to the total effective one-electron potential outside the surface. The advantage of this approach is that the quasiparticle interactions with electronic density fluctuations are represented by interactions with bosonic excitations (cf. Fig. 14 in Ref. [51]) and that the image potential-supported surface bands are already included in the unperturbed one-electron Hamiltonian of the system, H_0, which makes the computations of excited quasiparticle dynamics tractable. However, since the image potential derives from the adiabatic component of electron self-energies arising from the same electronic response, to avoid overcounting the interaction U_{im} should be subtracted from the effective interaction of quasiparticles with the electronic response. In this formulation the dynamics of electrons in surface bands is described by the total Hamiltonian

$$H = H_0 + H_{bath} + (V - U_{im}), \quad (14)$$

where H_{bath} describes the free field of electronic excitations constituting the spectrum of linear electronic response of the system (i.e. the spectrum of χ), and V describes the coupling of quasiparticles in

[3] The principle of *electron injection* into empty states of a system implies temporal boundary conditions in which the quasiparticle interactions with the system are switched on nonadiabatically. Besides the use of this principle in specific formulations of electron dynamics in terms of quasiparticle propagators [54], it has also been employed in the interpretations of 2PPE experiments from surface bands [55] and in semiclassical treatments of hyperthermal desorption of reaction products [56]. The opposite case of adiabatic switching on and off the interactions is more appropriate to the formulations of surface scattering theory, be the interactions treated quantum-mechanically [57] or semiclassically [58].

surface bands to these excitations. In this fashion the temporal effects associated with the formation of image potential appear as a *transient phase*

$$\varphi_b(t) = \phi_b(t) - E_b t \tag{15}$$

of the quasiparticle propagators (8) and (9) renormalized through the effective interaction

$$V' = (V - U_{im}). \tag{16}$$

This procedure is discussed in detail in Sec. II.B. of Ref. [51]. Analogous problem of subtraction of the static component of exchange and correlation energy from quasiparticle energies in bulk bands was discussed in Ref. [60].

Fig. 2 shows the survival probabilities (12) of initial states of an electron excited in the IS-band and a hole excited in the SS-band in the first step of 2PPE from Cu(1 1 1) surface which has served as a paradigm for studying ultrafast quasiparticle dynamics in surface bands. The underlying model calculations of the effects of interaction V' on the propagation of quasiparticles are described in Ref. [51]. This model treats the intra- and interband transitions of excited hot quasiparticles on the same footing but incorporates only the Cu conduction band and not the d-band electrons in screening processes. Also shown for comparison in the plots are the decays of quasiparticle survival probabilities

$$L_b^{\mathrm{FGR}}(t) = \exp(-\Gamma_b t), \tag{17}$$

which are governed by the Fermi golden rule-like (FGR) transition rates Γ_b that can be extracted from the fits of survival probabilities to steady state exponential decay in the same interval [51]. These results clearly illustrate strong deviations of the early evolution of initial quasiparticle states from the adiabatic or Markovian decay (17). In the present model the deviations arise mainly from virtual plasmon excitation within the Heisenberg uncertainty window before the on-the-energy-shell quasiparticle scattering by electron-hole excitations described by Γ_b in (17) sets in. However, in real copper the dominant contribution to the long wavelength limit of surface excitation spectrum will not come from plasmons but from vertical d → s,p band transitions (cf. Fig. 2 in Ref. [61]) that couple to excited hot quasiparticles.

Fig. 3 shows the early evolution of transient phases of electrons and holes excited into the IS- and SS-band, respectively, and propagating under the influence of interaction V'. Their behaviors are

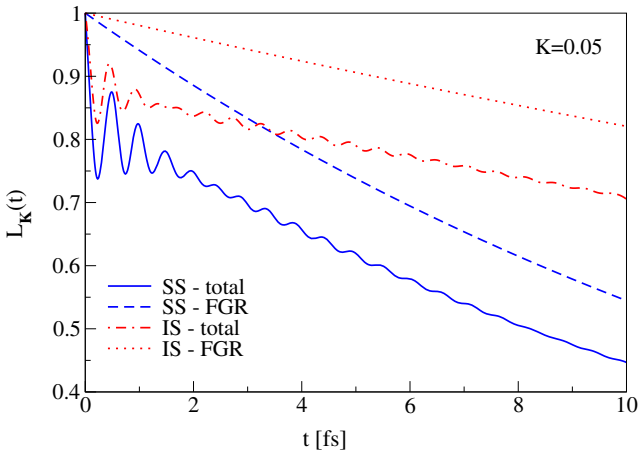

Fig. 2. Survival probabilities $L_{\mathbf{K}\,\mathrm{IS}}(t)$ and $L_{\mathbf{K}\,\mathrm{SS}}(t)$ for an electron and a hole after their promotion into the first image potential and surface state bands on Cu(1 1 1), respectively, with initial state wavevector $K = 0.05$ a.u. corresponding to initial $E_K^{\mathrm{IS}} = 37$ meV and $E_K^{\mathrm{SS}} = 60$ meV above the respective band bottom. Also shown for comparison are the Markovian decays of IS-electron and SS-hole as described by exponential law (17) with the corresponding FGR transition rates (see legend for assignments).

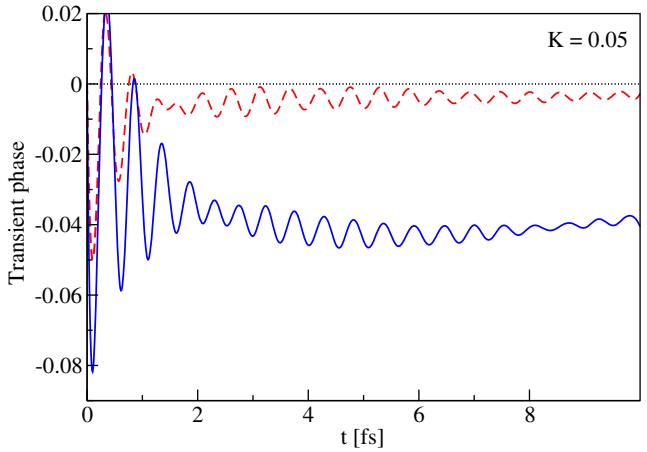

Fig. 3. Initial phase transients $\varphi_{\mathbf{K}}(t) = \phi_{\mathbf{K}}(t) - E_{\mathbf{K}}t$ for an electron and a hole promoted into the first IS- and SS-bands on Cu(1 1 1), dashed and full lines, respectively, with initial state wavevector $K = 0.05$ a.u.

dominantly determined by the virtual surface plasmon excitations and hence they measure the speed of formation of the screening or image potential induced by charged quasiparticles promoted into the surface localized states. Likewise the survival probabilities, these phase transients undergo fast variations during the early quasiparticle evolution before reaching the saturation values.

3.2. Effects of quasiparticle interactions with random adsorbates

Another ubiquitous interaction that the quasiparticles are subjected to upon their excitation into surface bands arises from the presence of localized defects on the surface. A paradigmatic system in this context is the Cu(1 0 0) surface covered with low concentration of Cu adsorbates. The dynamics of electron–adsorbate scattering in the IS-band on Cu(1 0 0) has been extensively studied in 2PPE experiments [31–36] and theoretically interpreted in the various formulations of single scattering center models [62–66]. Here we present the results for survival probabilities and phase relaxations of electrons excited into the first IS-band on Cu(1 0 0) surface in which they are scattered by the dipolar potentials of randomly distributed Cu adatoms [67]. In view of the long range character of electron–adsorbate dipolar interactions and relatively low initial quasiparticle energies in the range ~100 meV above the IS-band bottom we consider only the intraband scattering processes.

Fig. 4 shows the survival probability of an electron injected with the initial kinetic energy of 100 meV into the first IS-band on Cu(1 0 0) surface with low coverage of Cu adatoms $\Theta = 0.7\%$. Here the early evolution is described by the quadratic or "Zeno decay"

$$L_b(t) \approx 1 - t^2/\tau_Z^2 + \mathcal{O}(t^4), \tag{18}$$

which arises from the Heisenberg uncertainty for very short propagation times. Here the "Zeno time" is given by $\tau_Z^{-2} = (\mu_2 - \mu_1^2)$ where μ_1 and μ_2 are the first and second energy moments of the quasiparticle spectrum, respectively [68]. This is a universal behavior which occurs also in Fig. 2 but there it is quickly overtaken by virtual plasmon excitation on a sub-femtosecond time scale. As shown in the inset in Fig. 4, for longer times the Zeno decay evolves smoothly into intermediate FGR-like decay well approximated by the exponential law (17). For yet longer times exceeding 2000 fs this is followed by a crossover to asymptotic regime described by a combined inverse logarithm and power law decay [67].

Fig. 5 shows the total phase (13) of an electron injected into the first IS-band on Cu(1 0 0) with the initial kinetic energy of 100 meV. Here the drastic phase change in the same crossover region appears as a result of strong interferences among contributions to

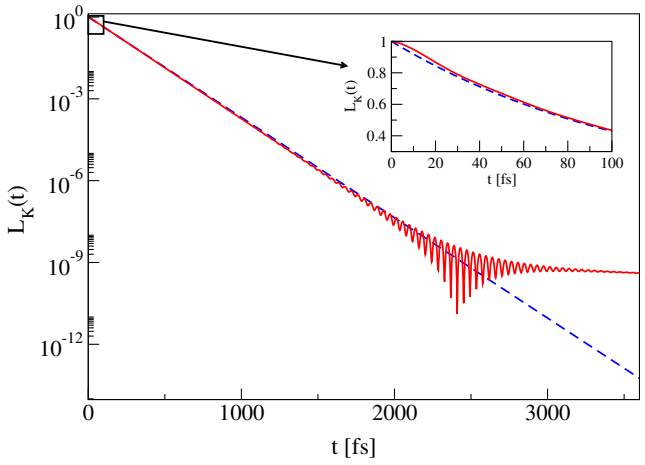

Fig. 4. Survival probability of an electron after excitation into IS-band on Cu(100) surface with low coverage $\Theta = 0.7\%$ of Cu adatoms, shown as a function of time in fs. The initial electron momentum K corresponds to energy $E_{\mathbf{K}} = 100$ meV. Dashed curve is the bare FGR decay of the form (17) with Γ_b describing elastic IS-electron scattering from adsorbates at low coverage $\Theta = 0.7\%$. Note logarithmic scale on the vertical axis. Here a strong interference between exponential and postexponential dephasings that cause survival collapse extend over the interval 1750 fs $\leqslant t \leqslant$ 3250 fs. Inset shows the early "Zeno" decay described by Eq. (18), with calculated $\tau_Z = 18.5$ fs.

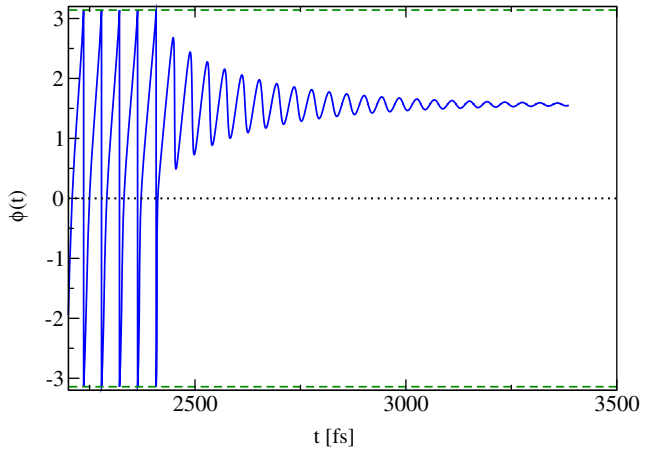

Fig. 5. Evolution of the total phase $\phi_{\mathbf{K}}(t)$ (modulo 2π) of the survival amplitude [see Eqs. (9) and (13)] of an electron after its excitation into IS-band on Cu(100) surface with low coverage of Cu adatoms $\Theta = 0.7\%$. The initial electron energy is $E_{\mathbf{K}} = 100$ meV. In the displayed range 2200 fs $\leqslant t \leqslant$ 3000 fs the corresponding survival probability (cf. Fig. 4) exhibits a survival collapse and crossover from the FGR to nonexponential asymptotic decay. The quasiparticle phase first grows linearly with time as $-i\phi(t) = -iE_{\mathbf{K}}t$ but in the shown crossover interval starts oscillating around a finite asymptotic value. In this interval the initial quasiparticle identity is lost.

the phase from different parts of the quasiparticle spectrum and signifies that simple quasiparticle features, viz. its energy and lifetime described within the FGR approach, are lost beyond that interval. Hence, for the here discussed kinetic parameters and strengths of electron–adsorbate interactions the "FGR window" of quasiparticle identity or its lifespan extends in the interval from around ~20 fs to ~1500 fs, which is well accessible to ultrafast electron spectroscopies.

4. Parameterization of ultrafast quasiparticle dynamics in surface bands: Application to 2PPE

The various aspects of ultrafast quasiparticle dynamics in surface bands presented in the preceding section illustrate that the application of time resolved pump-probe spectroscopies in assessments of quasiparticle features should be tuned across the time windows typical of Markovian evolution in which these features are most clearly discernible and thereby detectable. According to the results displayed in Figs. 2–5) these would be the intervals extending from around few tens of fs to around 1000 fs in which the evolution of quasiparticles is characterized by the FGR-type of decay and negligibly varying or stationary phase. Outside these intervals the experiments will also probe the non-Markovian early and asymptotic quasiparticle evolution. The extent to which these effects may manifest themselves in the measured spectra depends on interplays between the characteristics of pump and probe pulses and relaxation processes caused by photoexcitations in the probed system.

In this section we consider a simple parameterization of excited quasiparticle dynamics that could be used in the interpretation of ultrafast experiments. From what has been said above this may be feasible only in the FGR or Markovian time window in which the excitations retain a quasiparticle identity over a long enough and experimentally resolved temporal interval. Writing the quasiparticle propagators in this window in the form

$$G_b(t) \approx Z_b \exp\left[\mp iE_b t - \frac{1}{2}\Gamma_b t \mp i\varphi_b\right], \tag{19}$$

where Z_b^2 is the quasiparticle weight in the considered interval and the sign $\mp$ applies to electron and hole case, respectively, we may simulate the 1PPE and 2PPE amplitudes for given characteristics of excitation pulses determining the perturbing fields $E(t)$ in (6) and (7).

A widely used approach for simulating the 2PPE spectra from surface bands is based on few-level models in which single electron dynamics is described in the framework of optical Bloch equations [22,23,30,43,45–47] (OBE) involving the Markovian approximation for quasiparticle dynamics. However, a theoretical clue as to the origin of phenomenological parameters appearing in the OBE damping matrix $\widehat{\mathbf{\Gamma}}$ [cf. Eq. (6) in Ref. [45]] pertinent to 2PPE from surfaces has not been provided so far. Using the approach described in Sections 2 and 3, and expressions (4) and (7) with the Markovian limit of quasiparticle propagators (19), we can establish a mapping between the parameters entering expression (19) and the elements of $\widehat{\mathbf{\Gamma}}$ introduced in simulations of 2PPE final state populations by the OBE. To this end we first note that the standard OBE modeling of optically induced inter-level (interband) transitions of electrons in a system with discrete energy spectrum is based on the one-particle description of electron evolution obeying the Markovian regime. In this picture only the excited electron decay and dephasing rates determine the matrix elements of $\widehat{\mathbf{\Gamma}}$. However, as in 2PPE experiments from surface bands the holes excited by the pump pulse propagate and decay simultaneously with the photoexcited electrons, their evolution is "backfolded" onto the electronic evolution in the intermediate and final states of the 2PPE amplitude [41,42] [cf. Fig. 1 and Eq. (7)]. Thus, in a 3-level model comprising the initial ground state of the system (level 1), the excited IS-electron-SS-hole intermediate state (level 2), and the 2PPE final f-electron-SS-hole state (level 3), the total decay rates are given by 0, $\Gamma_{IS} + \Gamma_{SS}$ and $\Gamma_f + \Gamma_{SS}$, respectively, etc. These features must be included in the $\widehat{\mathbf{\Gamma}}$ matrix that should now describe evolution of the optically excited electron-hole pair in an open many-body system in which besides the electron also the photoexcited hole decays. Assuming $\Gamma_f = 0$ and stationary phases $\varphi_b(t) = \varphi_b$ in (19) during the considered interval, we obtain for $\widehat{\mathbf{\Gamma}}$ in the 3-level model:

$$\widehat{\mathbf{\Gamma}} = \begin{pmatrix} 0 & \frac{\Gamma_{SS}+\Gamma_{IS}}{2} & \frac{1}{2}\Gamma_{SS} \\ \frac{\Gamma_{SS}+\Gamma_{IS}}{2} & (\Gamma_{SS}+\Gamma_{IS}) & \frac{2\Gamma_{SS}+\Gamma_{IS}}{2} \\ \frac{1}{2}\Gamma_{SS} & \frac{2\Gamma_{SS}+\Gamma_{IS}}{2} & \Gamma_{SS} \end{pmatrix}. \tag{20}$$

Here Γ_{SS} and Γ_{IS} can be determined from interpolations of the quasiparticle survival probabilities in the FGR-window (cf. Figs. 2 and 4).

In the following we shall demonstrate the equivalence of calculations of 2PPE populations (7) using Markovian limits of quasiparticle propagators (19) and the OBE simulations based on $\widehat{\Gamma}$ defined by (20) and in the rotating wave approximation. To simulate the spectra corresponding to normal 2PPE from SS- and IS-bands on Cu(1 1 1) we first extrapolate the values of Γ_{ii} from the corresponding survival probabilities fitted to the form (19) so as to reproduce the *early decay* of IS-electron and SS-hole photoexcited at the respective band bottoms. This yields the values $\Gamma_{SS} = 16$ meV and $\Gamma_{IS} = 21$ meV that are slightly lower than the ones calculated in adiabatic theories [39], viz. $\Gamma_{SS} = 21$ meV and $\Gamma_{IS} = 23$ meV, which also take into account the role of the d-band screening and quasielastic quasiparticle scattering by phonons. Using the latter corrected values we carry out calculations of the spectra for 2PPE from the bottom of SS-band on Cu(1 1 1) surface at $E^{SS}_{\mathbf{K}=\mathbf{0}} - E_V = -5.25$ eV, via the IS-band intermediate state at $E^{SS}_{\mathbf{K}=\mathbf{0}} - E_V = -0.7$ eV. The full-width-at-half-maximum (FWHM) of the Gaussian pump ($\omega_{pu} = 4.2$ eV) and Gaussian probe ($\omega_{pr} = 2.1$ eV) pulses of unit amplitude is $T_p = 10$ fs, and the delay times τ_{2PPE} exceeding 20 fs for which the Markovian form (19) already represents a good approximation to the quasiparticle propagators.

The results of simulations in the two approaches differ within the numerical accuracy only by the normalization factors and hence are shown as single plots in Fig. 6 for the pump and probe delay times of 21, 23 and 25 fs for which the redistribution of spectral weight from the direct peak at photoelectron kinetic energy $E_k = E_f - E_V = 1.05$ eV to the indirect peak at $E_k = 1.4$ eV takes place. It is seen that for such short duration of excitation pulses the observation of the two peak structure in 2PPE spectra from surface bands on Cu(1 1 1) may be rather critical. The obtained results clearly demonstrate the equivalence of 2PPE spectra obtained from the above described time-dependent perturbation theory approach constrained to the Markovian regime and from OBE simulations based on the parameters extracted from the results of perturbation theory. In this respect the 2PPE spectra obtained from the thus parameterized OBE simulations appear as the simplest approximation to the full expression for the population density (3) in which the effects of early transients and asymptotic evolutions of quasiparticles have been neglected. This restricts the application of this approach to descriptions of 2PPE which measures the intermediate FGR-regime of quasiparticle evolutions that extends past the early transients ($\geqslant$10–20 fs for the examples studied in Section 3) up to the onsets of collaps of quasiparticle survival probability and phase. The duration of this interval, or the quasiparticle lifespan, depends on the strength of quasiparticle interactions with the environment. Hence, in view of what has been established in this and preceding section, theoretical interpretations of time resolved and interferometric 2PPE measurements utilizing ultrashort pulses of few fs duration and small delays require the treatments going beyond the validity of Markovian approximation and OBE modeling.

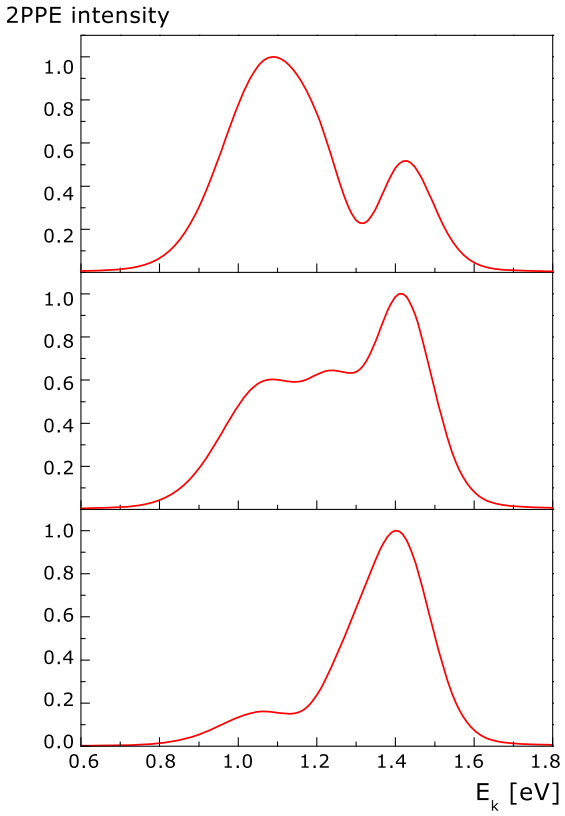

Fig. 6. Simulations of final state population intensities in normal 2PPE from SS-band on Cu(1 1 1) surface via the intermediate IS-state band shown as the functions of photoelectron kinetic energy E_k. The spectra were obtained from Markovian limit of expression (7) and from the optical Bloch equations with parameterization (20). For the parameters of pump and probe Gaussian pulses,band energies and decay rates see text. Top: 2PPE spectrum as function of photoelectron final energy above the vacuum level for the pulse delay $\tau_{2PPE} = 21$ fs. Center: same for $\tau_{2PPE} = 23$ fs. Bottom: same for $\tau_{2PPE} = 25$ fs. The spectra from the two approaches differ only by constant factors and are shown as single plots normalized to maximum peak intensities.

5. Summary

In this short review we have outlined several important manifestations of ultrafast dynamics and relaxation of hot charge carriers which may affect the spectra of photoelectrons emitted from surface bands in time resolved optical pump-probe experiments. We have first established essentially exact time dependent formalism for calculating photoemission amplitudes and the final state photoelectron populations in 1PPE, 2PPE and interferometric 2PPE from occupied states in surface bands and then singled out expressions describing the processes which give leading contributions to the photoelectron yield. These expressions have simple representations in terms of the propagators of quasiparticles and their coupling to the electromagnetic fields of pump and probe pulses, and as such enable the analyses of the effects of both the hot charge carrier dynamics and pulse characteristics on the measured photoelectron spectra. We have specifically discussed the nonadiabatic features and relaxation inherent to excited charge carrier propagation in surface bands during the initial, intermediate and final stages of 2PPE and pinpointed the intervals of Markovian dynamics in which case a conceptually simple quasiparticle description of photoemission is possible. Since this is also the interval of validity of 2PPE final state population modeling by the OBE, we were able to establish a mapping between the two descriptions and thereby determine the elements of the so far phenomenologically treated OBE damping matrix by making use of the results of earlier first principles calculations of decay and dephasing rates.

However, our approach of modeling the time resolved photoelectron spectra is not restricted to the Markovian approximation for quasiparticle dynamics but allows also the studies of 2PPE and interferometric 2PPE in other regimes in which due to the short duration of pump and probe pulses and their delays the above discussed nonadibatic and transient effects may significantly influence the measured spectra. These aspects of ultrafast spectroscopies will be addressed in the forthcoming work.

References

[1] G. Ertl, H. Knözinger, F. Schüth, J. Weitkamp (Eds.), Handbook of Heterogeneous Catalysis, Wiley-VCH, 2008.
[2] T.N. Rhodin, G. Ertl (Eds.), Nature of the Surface Chemical Bond, Elsevier Science, Amsterdam, 1979.
[3] T. Matsushima, Progr. Surf. Sci. 82 (2007) 435.
[4] Anders Nilsson, Lars G.M. Pettersson, Jens Nørskov (Eds.), Chemical Bonding at Surfaces and Interfaces, Elsevier, Amsterdam, 2008.
[5] B. Gumhalter, K. Wandelt, Ph. Avouris, Phys. Rev. B 37 (1988) 8048.
[6] P.M. Echenique, J.B. Pendry, J. Phys. C 11 (1978) 2065.
[7] M. Wolf, G. Ertl, Science 288 (2000) 1352.
[8] S.D. Kevan, R.H. Gaylord, Phys. Rev. B 36 (1987) 5809.
[9] R. Paniago, R. Matzdorf, G. Meister, A. Goldmann, Surf. Sci. 336 (1995) 113.
[10] A. Goldmann, R. Matzdorf, Progr. Surf. Sci. 42 (1993) 331; R. Matzdorf, Surf. Sci. Rep. 30 (1998) 153.
[11] P. Heimann, H. Neddermeyer, H.F. Roloff, J. Phys. C: Solid State Phys. 10 (1977) L17.
[12] F. Reinert, G. Nicolay, S. Schmidt, D. Ehm, S. Hüfner, Phys. Rev. B 63 (2001) 115415.
[13] F. Dose, Surf. Sci. Rep. 5 (1985) 337. and references therein.
[14] J. Li, W.-D. Schneider, R. Berndt, O.R. Bryant, S. Crampin, Phys. Rev. Lett. 81 (1998) 4464.
[15] L. Bürgi, O. Jeandupeux, H. Brune, K. Kern, Phys. Rev. Lett. 82 (1999) 4516; L. Vitali, P. Wahl, M.A. Schneider, K. Kern, V.M. Silkin, E.V. Chulkov, P.M. Echenique, Surf. Sci. 523 (2003) L47.
[16] R. Haight, Surf. Sci. Rep. 21 (1995) 275.
[17] E. Bertel, Surf. Sci. 331 (1995) 136.
[18] T. Fauster, W. Steinmann, in: P. Halevi (Ed.), Electromagnetic Waves: Recent Developments in Research, vol. 2, North Holland, Amsterdam, 1995, p. 347.
[19] T. Hertel, E. Knoesel, M. Wolf, G. Ertl, Phys. Rev. Lett. 76 (1996) 535.
[20] M. Wolf, E. Knoesel, T. Hertel, Phys. Rev. B 54 (1996) R5295.
[21] M. Wolf, Surf. Sci. 377–379 (1997) 343.
[22] M. Wolf, A. Hotzel, E. Knoesel, D. Velic, Phys. Rev. B 59 (1999) 5926.
[23] H. Petek, S. Ogawa, Progr. Surf. Sci. 56 (1997) 239.
[24] S. Ogawa, H. Nagano, H. Petek, A.P. Heberle, Phys. Rev. Lett. 78 (1997) 1339.
[25] H. Petek, A.P. Heberle, W. Nessler, H. Nagano, S. Kubota, S. Matsunami, N. Moriya, S. Ogawa, Phys. Rev. Lett. 79 (1997) 4649.
[26] H. Petek, H. Nagano, S. Ogawa, Phys. Rev. Lett. 83 (1999) 832.
[27] J. Güdde, M. Rohleder, T. Meier, S.W. Koch, U. Höfer, Science 318 (2007) 1287.
[28] U. Höfer, I.L. Shumay, C. Reuss, U. Thomann, W. Wallauer, T. Fauster, Science 277 (1997) 1480.
[29] Ch. Reuss, I.L. Schumay, U. Thomann, M. Kutschera, M. Weinelt, Th. Fauster, Phys. Rev. Lett. 82 (1999) 153.
[30] M. Weinelt, J. Phys.: Condens. Matter 14 (2002) R1099.
[31] T. Hertel, E. Knoesel, E. Hasselbrink, M. Wolf, G. Ertl, Surf. Sci. 317 (1994) L1147.
[32] K. Boger, M. Weinelt, Th. Fauster, Phys. Rev. Lett. 92 (2004) 126803.
[33] K. Boger, M. Weinelt, J. Wang, Th. Fauster, Appl. Phys. A 78 (2004) 161.
[34] K. Boger, Th. Fauster, M. Weinelt, New J. Phys. 7 (2005) 110.
[35] Th. Fauster, M. Weinelt, U. Höfer, Progr. Surf. Sci. 82 (2007) 224.
[36] S. Smadici, R.M. Osgood, Phys. Rev. B 71 (2005) 165424.
[37] P.M. Echenique, J.M. Pitarke, E.V. Chulkov, A. Rubio, Chem. Phys. 251 (2000) 1.
[38] P.M. Echenique, R. Berndt, E.V. Chulkov, Th. Fauster, A. Goldman, U. Höfer, Surf. Sci. Rep. 52 (2004) 219.
[39] E.V. Chulkov, A.G. Borisov, J.P. Gauyacq, D. Sánchez-Portal, V.M. Silkin, V.P. Zhukov, P.M. Echenique, Chem. Rev. 106 (2006) 4160.
[40] H. Ueba, Surf. Sci. 334 (1995) L719.
[41] M. Sakaue, T. Munakata, H. Kasai, A. Okiji, Phys. Rev. B 66 (2002) 094302; M. Sakaue, T. Munakata, H. Kasai, A. Okiji, Phys. Rev. B 68 (2003) 205421; M. Sakaue, T. Munakata, H. Kasai, A. Okiji, Surf. Sci. 532–535 (2003) 30.
[42] M. Sakaue, J. Phys.: Condens. Matter 17 (2005) S245.
[43] H. Ueba, B. Gumhalter, Progr. Surf. Sci. 82 (2007) 193.
[44] C. Timm, K.H. Bennemann, J. Phys.: Condens. Matter 16 (2004) 661.
[45] K. Boger, M. Roth, M. Wainelt, Th. Fauster, P.-G. Reinhard, Phys. Rev. B 65 (2002) 075104.
[46] T. Klamroth, P. Saalfrank, U. Höfer, Phys. Rev. B64 (2001) 035420.
[47] H. Ueba, T. Mii, Appl. Phys. A 71 (2000) 537.
[48] N.W. Ashcroft, W.L. Schaich, Phys. Rev. B 3 (1971) 2452.
[49] C. Caroli, D. Lederer-Rozenblatt, B. Roulet, D. Saint-James, Phys. Rev. B 8 (1973) 4552.
[50] J. Pendry, Surf. Sci. 57 (1976) 679.
[51] P. Lazić, V.M. Silkin, E.V. Chulkov, P.M. Echenique, B. Gumhalter, Phys. Rev. B 76 (2007) 045420.
[52] J.J. Chang, D.C. Langreth, Phys. Rev. B5 (1972) 3512; J.J. Chang, D.C. Langreth, Phys. Rev. B8 (1973) 4638.
[53] F. El-Shaer, B. Gumhalter, Phys. Rev. Lett. 93 (2004) 236804.
[54] S. Doniach, E.H. Sondheimer, Green's Functions for Solid State Physicists, W.A. Benjamin, Inc., Reading, Massachusets, 1974. Chapter 5.
[55] A. Winkelmann, F. Bisio, R. Ocaña, W.-C. Lin, M. Nývlt, H. Petek, J. Kirschner, Phys. Rev. Lett. 98 (2007) 226601.
[56] B. Gumhalter, T. Matsushima, Surf. Sci. 561 (2004) 183.
[57] B. Gumhalter, Phys. Rep. 351 (2001) 1.
[58] A. Bilić, B. Gumhalter, W. Mix, A. Golichowski, S. Tzanev, K.J. Snowdon, Surf. Sci. 307–309 (1994) 165; W. Mix, S. Tzanev, A. Golichowski, K.J. Snowdon, A. Bilić, B. Gumhalter, Surf. Sci. 331–333 (1995) 332; A. Bilić, B. Gumhalter, K.J. Snowdon, Surf. Sci. 368 (1996) 71.
[59] P. Lazić, V.M. Silkin, E.V. Chulkov, P.M. Echenique, B. Gumhalter, Phys. Rev. Lett. 97 (2006) 086801.
[60] W. Ekardt, W.-D. Schöne, R. Keyling, Appl. Phys. A 71 (2000) 529; W.-D. Schöne, Progr. Surf. Sci. 82 (2007) 161.
[61] D. Lovrić, B. Gumhalter, Phys. Rev. B 38 (1988) 10323.
[62] A.G. Borisov, A.K. Kazansky, J.P. Gauyacq, Phys. Rev. B 65 (2002) 205414.
[63] A.G. Borisov, J.P. Gauyacq, A.K. Kazansky, Surf. Sci. 540 (2003) 407.
[64] F.E. Olsson, M. Persson, A.G. Borisov, J.P. Gauyacq, J. Lagoute, S. Fölsch, Phys. Rev. Lett. 93 (2004) 206803.
[65] F.E. Olsson, A.G. Borisov, M. Persson, N. Lorente, A.K. Kazansky, J.P. Gauyacq, Phys. Rev. B 70 (2004) 205417.
[66] F.E. Olsson, A.G. Borisov, J.P. Gauyacq, Surf. Sci. 600 (2006) 2184.
[67] B. Gumhalter, A. Šiber, H. Buljan, Th. Fauster, Phys. Rev. B 78 (2008) 155410.
[68] E. Rufeil Fiori, H.M. Pastawski, Chem. Phys. Lett. 420 (2006) 35; E. Rufeil Fiori, H.M. Pastawski, Braz. J. Phys. 36 (3B) (2006) 844.